Enhancement in Research Octane Number and Hydrogen Production via Dynamic Optimization of a Novel Spherical Axial−Flow Membrane Naphtha Reformer

ARTICLE *in* INDUSTRIAL & ENGINEERING CHEMISTRY RESEARCH · DECEMBER 2011

Impact Factor: 2.59 · DOI: 10.1021/ie2010912

4 AUTHORS, INCLUDING:

M. R. Rahimpour
Shiraz University
331 PUBLICATIONS **3,013** CITATIONS
SEE PROFILE

Davood Iranshahi
Amirkabir University of Technology
50 PUBLICATIONS **390** CITATIONS
SEE PROFILE

Ehsan Pourazadi
University of Sydney
27 PUBLICATIONS **314** CITATIONS
SEE PROFILE

I&EC research
Industrial & Engineering Chemistry Research

ARTICLE

pubs.acs.org/IECR

Enhancement in Research Octane Number and Hydrogen Production via Dynamic Optimization of a Novel Spherical Axial-Flow Membrane Naphtha Reformer

Mohammad Reza Rahimpour,* Davood Iranshahi, Khadijeh Paymooni, and Ehsan Pourazadi

Department of Chemical Engineering, School of Chemical and Petroleum Engineering, Shiraz University, Shiraz 71345, Iran

ABSTRACT: Spherical axial-flow membrane reactors (SMR) can be proposed as a promising alternative for conventional tubular reactors (CTR) in the catalytic naphtha reforming process. In this study, the operating conditions and design parameters of SMR are optimized via a differential evolution (DE) method to maximize the hydrogen yield, the reformate production rate, and the aromatic content of reformate (octane number). Regarding this, 26 decision variables such as the membrane thickness, catalyst mass distribution, and flow distribution of sweeping gas are optimized, and the performance of the SMR is evaluated under optimized operating conditions. The optimization results show that the operating costs can decrease sharply with a decrease in the sweeping gas streamlines' pressures where they decline from 985, 1810, and 2000 kPa in the first, the second, and the third reactors of nonoptimized SMR to 242.4, 563.1, and 796.6 kPa in optimized SMR, respectively. Moreover, the research octane number (RON) of gasoline can improve well in optimized SMR owing to the achievement of higher aromatic yield and the aromatic content of the reformate. Consequently, an optimized SMR configuration can properly address the increasing demand for high-octane gasoline. The superiority of the optimized SMR configuration to CTR can be counted as assisting the membrane concept, lower pressure drop along the reaction side, and utilizing the optimum operating conditions.

1. INTRODUCTION

1.1. Naphtha. Full-range naphtha is the fraction of the crude oil with boiling between 30 and 200 °C, and constitutes typically 15−30% by weight of the crude oil. This includes hydrocarbons ranging from C_5 to C_{12}, some sulfur, and small amounts of nitrogen. The composition of given naphtha depends on the type of crude oil, the boiling range of the naphtha, and whether it is obtained directly from crude oil distillation or produced by catalytic or thermal cracking of heavier oil fractions. A typical straight-run medium naphtha contains 40−70 wt % paraffins, 20−50 wt % naphthenes, 5−20 wt % aromatics, and only 0−2 wt % olefins. The purpose of catalytic reforming is primarily to increase the octane number of the naphtha feedstock to a level that makes the reformate product suitable as a gasoline blend stock.[1] The octane number represents the ability of a gasoline to resist knocking during combustion of the air−gasoline mixture in the engine cylinder. In practice two octane ratings are measured, the research octane number (RON) and the motor octane number (MON), which differ in test procedures used. RON represents the engine performance at low speed, whereas MON is a representative for high-speed driving.[2,3] Severe reaction conditions are required to reach a specific RON level. To optimize the hydrogen and aromatics formation (RON), refiners have to operate under sever conditions of high temperature and low hydrogen pressure. The former condition endangers the catalyst life by sintering, and the latter one aggravates the coking phenomenon on the catalyst surface. Therefore, this is a critical situation for refiners to make a wise decision and a good balance between the market demand (immediate need for high RON gasoline) and the possible operating (providing high temperature) and capital costs (catalyst lifetime). Actually, small variations in RON values can significantly influence the production economics.[1]

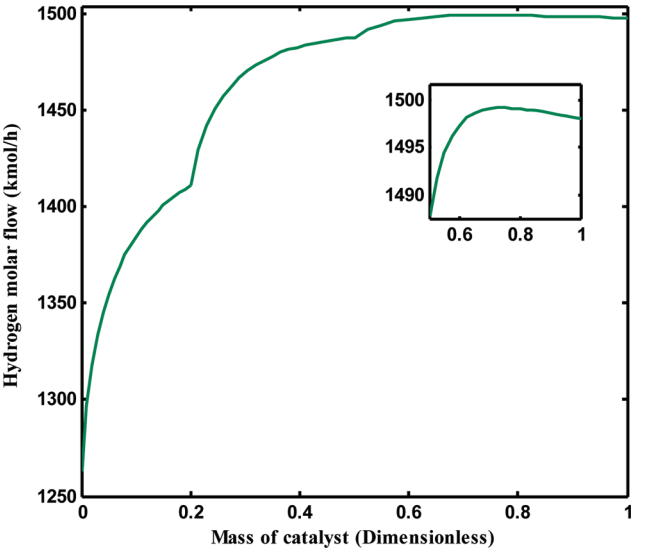

Figure 1. The hydrogen production rate along CTR.

1.2. Objectives. To eliminate the pressure drop problem and hydrogen consumption at the end of the third reactor in a

Received: May 21, 2011
Accepted: October 23, 2011
Revised: September 26, 2011
Published: October 24, 2011

dx.doi.org/10.1021/ie2010912 | *Ind. Eng. Chem. Res.* 2012, 51, 398–409

Table 1. The Area underneath the Reaction Rate Curves of CTR, SMR, and OSMR

reaction rates	1st reactor (kmol/(kg_{cat} h))	2nd reactor (kmol/(kg_{cat} h))	3rd reactor (kmol/(kg_{cat} h))	total areas (kmol/(kg_{cat} h))
		CTR		
The first reaction rate (r_1)	0.017	0.0065	0.0016	0.0250
The second reaction rate (r_2)	0.8273×10^{-3}	-0.0334×10^{-3}	-0.9587×10^{-3}	-0.1648×10^{-3}
The third reaction rate (r_3)	0.3280×10^{-3}	0.2011×10^{-3}	0.1075×10^{-3}	0.6366×10^{-3}
The fourth reaction rate (r_4)	0.0006	0.0013	0.0024	0.0043
		SMR		
The first reaction rate (r_1)	0.0172	0.0065	0.0017	0.0255
The second reaction rate (r_2)	0.0008	−0.0001	−0.0012	−0.0004
The third reaction rate (r_3)	0.3286×10^{-3}	0.1974×10^{-3}	0.1131×10^{-3}	0.6391×10^{-3}
The fourth reaction rate (r_4)	0.0006	0.0013	0.0027	0.0047
		OSMR		
The first reaction rate (r_1)	0.0212	0.0079	0.0015	0.0306
The second reaction rate (r_2)	0.0007	−0.0003	−0.0010	−0.0007
The third reaction rate (r_3)	0.4382×10^{-3}	0.2204×10^{-3}	0.0679×10^{-3}	0.7265×10^{-3}
The fourth reaction rate (r_4)	0.0009	0.0016	0.0021	0.0046

conventional tube reactor (CTR) (see Figure 1), the axial-flow spherical membrane reactor (SMR) was proposed in the previous study[4] to address these issues. In addition, refineries have been looking for ways to increase the gasoline octane number and hydrogen production rate due to restricted legislations on hydrotreating and desulfurization units.[5] Regarding this, the DE optimization method[6−8] is applied in the present study to optimize the operating conditions and design parameters of the spherical axial-flow membrane reactor (SMR) to boost hydrogen yield, reformate production rate, and the aromatic content of reformate (A comparison between the successful outcomes of optimized SMR such as higher hydrogen and aromatic production rates and the results of SMR and CTR are reported in Table 1). Twenty-six decision variables such as catalyst mass distribution, hydraulic diameters, inlet molar flow rate of the naphtha feed, membrane thickness, flow distribution of sweeping gas, and operating pressures, etc. are optimized via the DE approach to investigate the performance of the SMR under optimized operating conditions. Operating under optimized conditions significantly decreases the initial membrane fabrication cost by reducing the total membrane area in use where it significantly drops to almost 4 m^2 in the optimized SMR as compared with the nonoptimized SMR in addition to the remarkable decline of 51 m^2 compared with the same configuration of tubular membrane reactor (TMR). Furthermore, the feasibility of achieving higher gasoline RON (there is a linear relationship between RON and the aromatic fraction in the reformate[1]) and a negligible pressure drop and so forth in the optimized SMR configuration compared to that in the CTR are extensively discussed in the subsequent sections.

2. KINETIC EXPRESSIONS (SMITH'S MODEL)

To verify the feedstock or product qualities, it is often sufficient for the process engineers to know the PONA (paraffin, olefin, naphthene, and aromatic) group concentrations.[1] Accordingly, the Smith's model[9] is considered to simplify the complexity of feed stock. The following four reactions are considered in this model:

- Dehydrogenation of naphthenes to aromatics

$$\text{naphthenes } (C_nH_{2n}) \leftrightarrow \text{aromatics } (C_nH_{2n-6}) + 3H_2 \quad \Delta H = 71038.06 \text{ (kJ/kmol } H_2) \quad (1)$$

- Dehydrocyclization of paraffins to naphthenes

$$\text{naphthenes } (C_nH_{2n}) + H_2 \leftrightarrow \text{paraffins } (C_nH_{2n+2}) \quad \Delta H = -36953.33 \text{ (kJ/kmol } H_2) \quad (2)$$

- Hydrocracking of naphthenes to lower hydrocarbons

$$\text{naphthenes } (C_nH_{2n}) + n/3H_2 \rightarrow \text{lighter ends } (C_1-C_5) \quad \Delta H = -51939.31 \text{ (kJ/kmol } H_2) \quad (3)$$

- Hydro cracking of paraffins to lower hydrocarbons

$$\text{paraffins } (C_nH_{2n+2}) + (n-3)/3H_2 \rightarrow \text{lighter ends } (C_1-C_5) \quad \Delta H = -56597.54 \text{(kJ/kmol } H_2) \quad (4)$$

The related rate expressions and their constants were reported in the previous publication.[10] The corresponding reactions' rates for CTR are reported in Table 1. Despite a high volume hydrogen production in both first and the second reactors, the first reactor plays a significant role in hydrogen production. The second reaction proceeds readily in the reverse direction (i.e., dehydrocyclization reaction) in the second and the third reactors (the related rates are negative). Although the third reaction takes place in all three reactors, its reaction rate is not too high. Furthermore, the fourth reaction takes place mainly in the second and the third reactors. In general, dehydrogenation and isomerization are the main reactions in the first reactor while dehydrogenation, isomerization, cracking, and dehydrocyclization take place in the second reactor and cracking and dehydrocyclization reactions are the key reactions in the third reactor.

dx.doi.org/10.1021/ie2010912 |Ind. Eng. Chem. Res. 2012, 51, 398–409

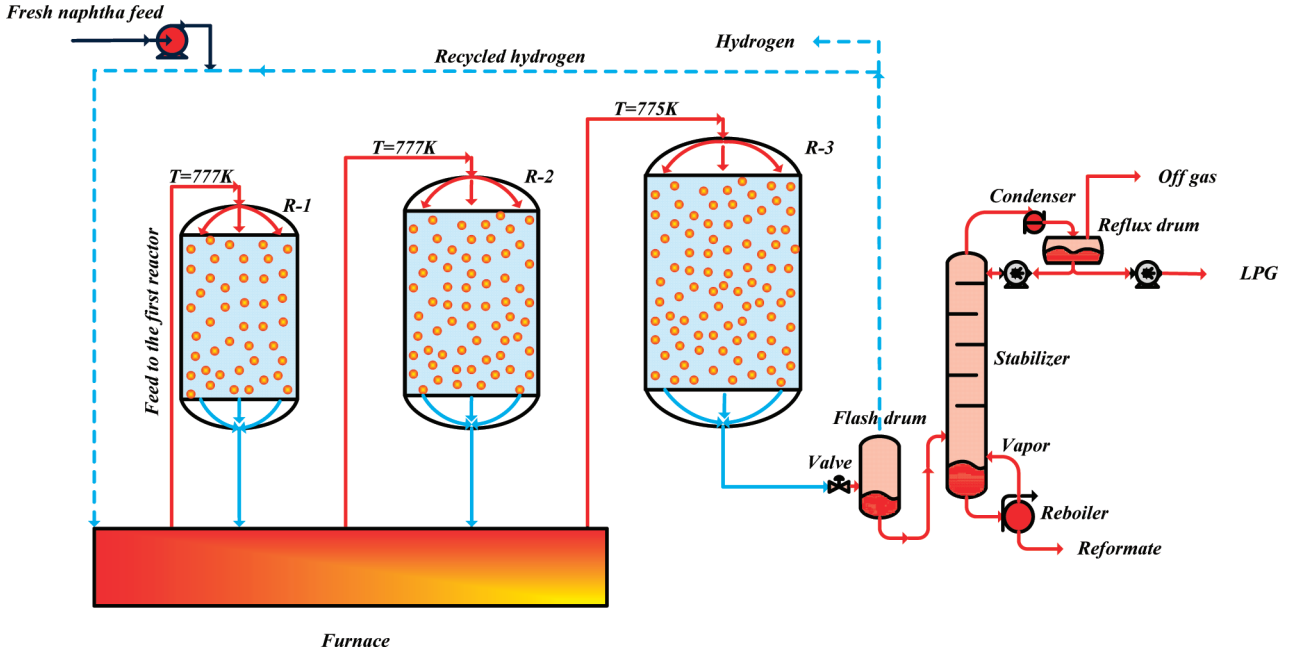

Figure 2. A simple process flow diagram for conventional tubular reactor (CTR).

3. PROCESS DESCRIPTION

A simplified process flow diagram for conventional tubular reactors (CTR) in naphtha reforming process is depicted in Figure 2.

Because of some disadvantages of CTR such as high pressure drop along the reactor, high manufacturing costs (twice thickness of tubular reactors compared with spherical reactors), and low production capacity due to high pressure drop, spherical reactors are proposed. A novel idea in spherical reactors is the feasibility of applying a membrane layer for hydrogen removal from the reaction side in order to shift the thermodynamic equilibrium to the products side. As the application of a membrane layer in radial-flow spherical reactors seems to be nearly impossible, the flow pattern in the spherical reactor was changed and consequently an axial-flow instead of a radial-flow pattern was proposed in the previous study.[4] A schematic diagram of SMR for naphtha reforming process is presented in Figure 3a. As shown in Figure 3b, SMR consists of two concentric spheres in which the surface of the inner sphere is coated with a hydrogen perm-selective membrane layer. According to Adhikari and Fernando[11] in most cases, self-supporting metallic membranes, especially Pd-based membranes, for hydrogen separation became unattractive because of their high cost, low permeance, and low chemical stability. Consequently, these membranes are generally prepared as thin films on porous support, which provides a mechanical support. Catalysts are situated in the inner sphere (tube side). The naphtha feed flows axially through the packed bed of the inner sphere (the catalytic bed is assumed to be homogeneous). The sweeping gas (which has a composition analysis similar to the recycled stream (0.695% hydrogen)) enters the outer sphere (shell side). Hydrogen is produced as a result of chemical reactions on catalysts' surfaces. Hydrogen permeates through the Pd−Ag membrane layer to the shell side and the sweeping gas carries the permeated hydrogen. According to the Le Chatelier's principle, the reaction is shifted toward the product side. Thus, higher products' yields (i.e., aromatics) are achieved in SMR in comparison with CTR. The cross sectional area of the inlet and the outlet of the inner sphere are smaller and it causes a severe pressure drop. Therefore, it is preferred to fill the space between two perforated screens with catalysts. Consequently, L/R ratio is defined as a decision variable during the optimization process of SMR. These perforated screens act as a mechanical support and cause more uniform feed distribution.

4. GOVERNING EQUATIONS

4.1. Mathematical Modeling. An element, composed of shell and tube sides, with the thickness of dz is taken into consideration. The naphtha feed with a flow rate of F_1 enters and reacts and eventually leaves the element of the inner sphere while hydrogen permeates through the membrane layer. The sweeping gas with a flow rate of F_2 enters and carries the permeated hydrogen and leaves the element of the outer sphere. The mass and energy balance equations obtained by analyzing this element are developed for both sides. They are coupled with the pressure drop correlation[12] and also thermodynamic and kinetic relations as well as auxiliary correlations for predicting the SMR performance. In this study, a homogeneous one-dimensional model has been taken into consideration. The results of the modeling section are reported in Table 2. The assumptions made for the mathematical modeling of SMR to reduce it to a one-dimensional model as well as the extensive explanations about this section can be found in the previous publication.[4] Furthermore, more details regarding CTR modeling were presented in the previous work.[13]

5. NUMERICAL SOLUTION

To solve the set of equations, a two-step procedure including a steady-state step followed by a dynamic one has been applied. The initial condition for the dynamic stage is achieved by solving the equation of the steady-state stage. In the steady-state procedure, all time variants are set to zero and the catalyst activity is considered to be 1. Thus, the results of the steady-state step are

dx.doi.org/10.1021/ie2010912 |Ind. Eng. Chem. Res. 2012, 51, 398–409

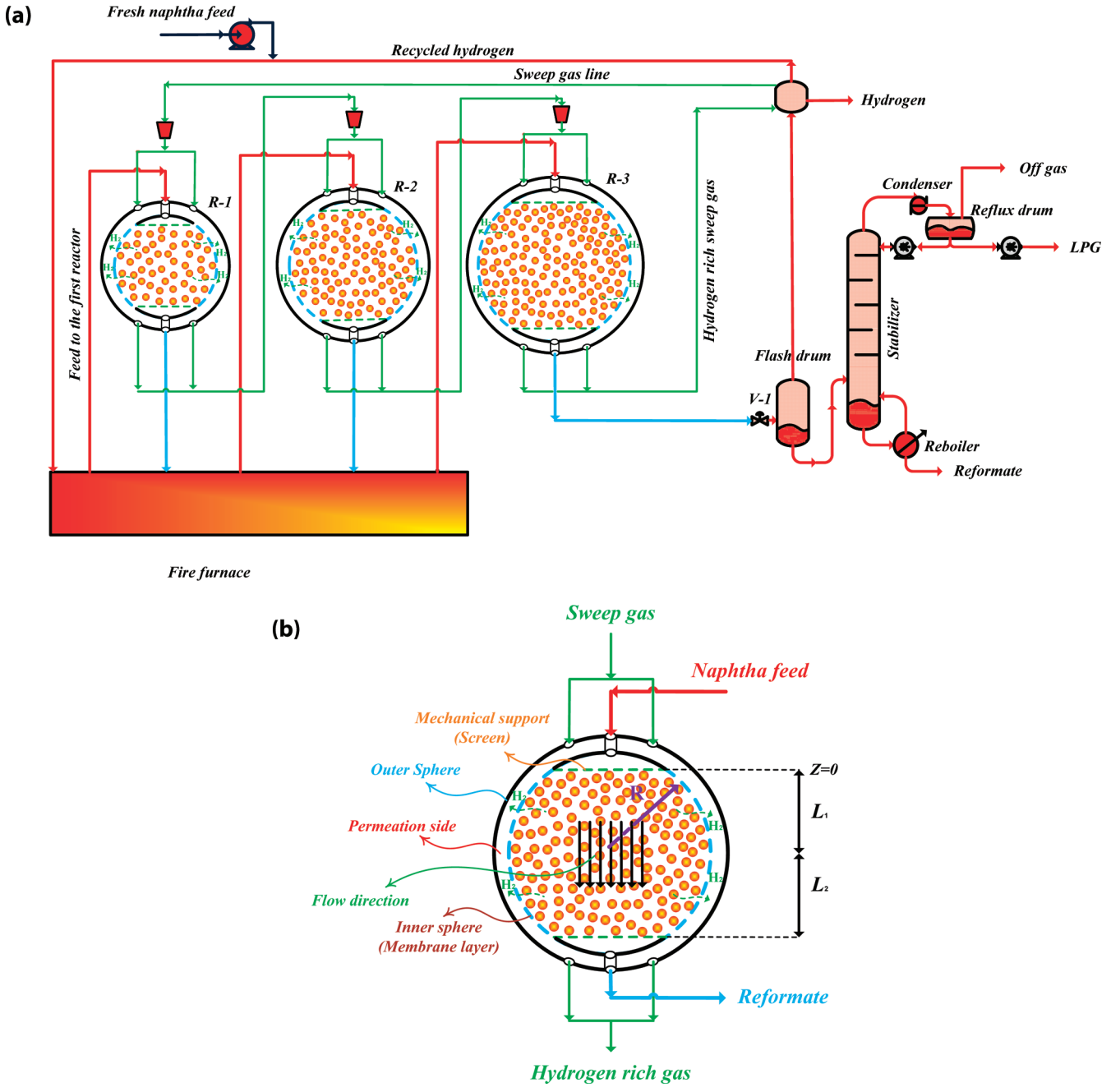

Figure 3. (a) Process flow diagram and (b) flow pattern of a spherical membrane reactor in catalytic naphtha reforming.

used as the initial conditions for the time-integration of the dynamic set of equations in each node through the reactor. This set of equations is solved by the orthogonal collocation method. More explanations concerning the orthogonal collocation method were presented in the previous work.[4]

6. VALIDITY OF MODEL

To verify the accuracy of the Smith's model in spite of considering simplified assumptions, the system of CTR is modeled and the achieved results are compared with the available plant data from a real industrial plant. Table 3 reports the plant data for CTR and predicted mole fractions of components at the output of the system for the steady-state condition. Analyses of components (paraffin, naphthene, and aromatic) are performed by the PONA test in a Stan Hop Seta apparatus. The aromatic is tested especially by ASTM 2159 equivalent to UOP 273 method.[14]

A satisfactory good agreement is observed between the daily observed plant data and modeling results under the unsteady-state condition for 800 operating days. The predicted values of the production rate, the corresponding observed data, and the residual error are reported in Table 4.

7. THE OPTIMIZATION PROBLEM

In this study, maximizing the sum of hydrogen yield, the reformate production rate, and the outlet aromatic content of reformate from the third reactor are considered in the

dx.doi.org/10.1021/ie2010912 |*Ind. Eng. Chem. Res.* 2012, 51, 398–409

Table 2. Mass and Energy Balances for Axial-Flow Spherical Reactor (SMR)

Fluid phase (Tube side)

$$D_{ej}\frac{1}{A_{c_1}}\frac{\partial}{\partial z}\left(A_{c_1}\frac{\partial C_j}{\partial z}\right)-\frac{1}{A_{c_1}}\frac{\partial(u_{z_1}A_{c_1}C_j)}{\partial z}+\rho_b a\sum_{i=1}^{m}v_{ij}r_i - \begin{cases}\frac{P_{per}}{A_{c_1}}J_{H_2} & j=H_2\\ 0 & j\neq H_2\end{cases} = \varepsilon\frac{\partial C_j}{\partial t}\quad j=1,2,...,n\quad i=1,2,...,m \tag{5}$$

$$C_T C_v \varepsilon\frac{\partial T}{\partial t}=RT\frac{\partial C_T}{\partial t}+k_{eff}\frac{1}{A_{c_1}}\frac{\partial}{\partial z}\left(A_{c_1}\frac{\partial T}{\partial z}\right)-u_z C_T C_p\frac{\partial T}{\partial z}+\rho_b\sum_{i=1}r_i\Delta H_i + J_{H_2}\frac{\beta P_{per}}{A_{c_1}}(H^t_{H_2}-\gamma_{H_2})+\frac{P_{per}U}{A_{c_1}}(T^s-T) \tag{6}$$

$$\beta = U_{HVS}(P^t_{H_2}-P^s_{H_2}) = \begin{cases}+1 & P^t_{H_2}\geq P^s_{H_2}\\ -1 & P^t_{H_2}<P^s_{H_2}\end{cases} \tag{7}$$

: Heaviside Function U_{HVS}

$$\gamma_{H_2}=(H^t_{H_2}-H^s_{H_2})U_{HVS}(P^t_{H_2}-P^s_{H_2})+H^s_{H_2}=\begin{cases}H^t_{H_2} & P^t_{H_2}\geq P^s_{H_2}\\ H^s_{H_2} & P^t_{H_2}<P^s_{H_2}\end{cases} \tag{8}$$

Fluid phase (Shell side)

$$D_{ej}\frac{1}{A_c}\frac{\partial}{\partial z}\left(A_c\frac{\partial C_j}{\partial z}\right)-\frac{1}{A_c}\frac{\partial(u_{z_1}A_c C_j)}{\partial z} + \begin{cases}\frac{P_{per}}{A_{c_1}}J_{H_2} & j=H_2\\ 0 & j\neq H_2\end{cases} = \varepsilon\frac{\partial C_j}{\partial t}\quad j=1,2,...,n\quad i=1,2,...,m \tag{9}$$

$$C_T C_v \varepsilon\frac{\partial T^s}{\partial t}=RT^s\frac{\partial C_T}{\partial t}+k_{eff}\frac{1}{A_c}\frac{\partial}{\partial z}\left(A_c\frac{\partial T^s}{\partial z}\right)-u_z C_T C_p\frac{\partial T^s}{\partial z} - J_{H_2}\frac{\beta P_{per}}{A_{c_1}}(H^t_{H_2}-\gamma_{H_2})-\frac{P_{per}U}{A_{c_1}}(T^s-T) \tag{10}$$

Hydrogen permeation rate

$$J_{H_2}=\frac{Q_0\exp(-\frac{E_{H_2}}{R_g T})}{\delta_{H_2}}(\sqrt{P^{tube}_{H_2}}-\sqrt{P^{shell}_{H_2}}) \tag{11}$$

$$Q_0=1.65\times10^{-5}molm^{-1}s^{-1}kPa^{\frac{-1}{2}},E_{H_2}=15.7kjmol^{-1}$$

Additional relations

$$A_{c_1}=\pi[R^2-(z-L_1)^2] \tag{12}$$

$$P_{per}=2\pi[R^2-(z-L_1)^2]^{0.5} \tag{13}$$

Boundary & initial conditions

$$z=0:\ C_j=C_{j0},\ T=T_0 \tag{14}$$

$$z=L_1+L_2:\ \frac{\partial C_j}{\partial z}=0,\ \frac{\partial T}{\partial z}=0 \tag{15}$$

$$t=0;C_j=C_j^{ss},T=T^{ss},T_s=T_s^{ss};a=1; \tag{16}$$

Ergun equation (Pressure drop)

$$\frac{dP}{dz}=\frac{150\mu}{\phi_s^2 d_p^2}\frac{(1-\varepsilon)^2}{\varepsilon^3}\frac{Q}{A_c}+\frac{1.75\rho}{\phi_s d_p}\frac{(1-\varepsilon)}{\varepsilon^3}\frac{Q^2}{A_c^2} \tag{17}$$

Catalyst deactivation

$$\frac{da}{dt}=-K_d\exp(-\frac{E_d}{R_g}(\frac{1}{T}-\frac{1}{T_R}))a^7 \tag{18}$$

$$T_R=770K,E_d=1.642\times10^5\ jmol^{-1},K_d=5.926\times10^{-5}h^{-1}$$

objective function.

$$\text{sum} = Y_{H_2} + R_{\text{ref}} + x_{\text{aromatics}} \tag{19}$$

Table 3. Comparison between Model Prediction and Plant Data for Fresh Catalyst

reactor no.	inlet temperature (K)	inlet pressure (kPa)	catalyst distribution (wt %)	input feedstock (mole %)	
1	777	3703	20	paraffin	49.3
2	777	3537	30	naphthene	36.0
3	775	3401	50	aromatic	14.7

	outlet temperature (K)				aromatic in reformate (mole %)			
no.	plant	AF-TR	SMR	OSMR	plant	AF-TR	SMR	OSMR
1	722	727.30	728.53	734.14		34.67	35.00	36.12
2	753	750.98	751.36	764.47		47.19	47.65	48.82
3	770	770.53	770.68	773.35	57.70	56.18	57.75	58.56

The below constraints are considered during the optimization process of SMR:

$$\frac{H_2}{HC}\geq 4.73 \tag{20}$$

$$\sum_{i=1}^{3}W_i = 1 \tag{21}$$

$$\sum_{i=1}^{3}N_i = 1 \tag{22}$$

$$P_1^{\text{in}} - P_3^{\text{out}} < 100\ \text{kPa} \tag{23}$$

where i represents the number of the reactors, W_i is the mass distribution of the catalysts in each reactor and N is the flow distribution of the sweeping gas in each reactor. P_1^{in} and P_3^{out} are the inlet pressure to the first reactor and the outlet pressure from the third reactor, respectively. Equation 23 implies that the pressure drop through the catalytic bed of SMR is slight.

The penalty function method is considered to eliminate the unacceptable results. This method involves penalizing the objective function in proportion to the extent of constraint violation (i.e., the penalty function takes a finite value when a constraint is violated and a value of zero when constraint is satisfied). In this study, the penalty parameter is considered as 10^7 however it may change from problem to problem. Finally, the objective function considered for minimizing this particular problem is as follows:

$$\text{result} = -\text{sum} + 10^7\left(\sum_{i=1}^{6}G_i^2\right) \tag{24}$$

where

$$G_1 = \max\left\{0,\left(4.73-\left(\frac{H_2}{Hc}\right)\right)\right\} \tag{25}$$

$$G_2 = \max\{0,(1.00001-(W_1+W_2+^2W_3))\} \tag{26}$$

$$G_3 = \max\{0,((W_1+W_2+^2W_3)-0.99999)\} \tag{27}$$

$$G_4 = \max\{0,((P_1^{\text{in}}-P_3^{\text{out}})-100)\} \tag{28}$$

$$G_5 = \max\{0,(1.00001-(N_1+^1N_2+N_3))\} \tag{29}$$

$$G_6 = \max\{0,((N_1+N_2+N_3)-0.99999)\} \tag{30}$$

dx.doi.org/10.1021/ie2010912 |Ind. Eng. Chem. Res. 2012, 51, 398–409

Table 4. Unsteady State Model Validation

time (day)	inlet temperature to the first reactor (K)	naphtha feed (ton/h)	plant (kmol/h)	AF-TR (model) (kmol/h)	devi % (model-plant/plant) × 100	SMR (kmol/h)	OSMR (kmol/h)
0	777.0	30.41	225.90	221.7819	−1.8230	219.10	226.19
34	777.3	30.41	224.25	222.7137	0.6851	220.08	227.22
62	777.8	31.00	229.65	228.1372	−0.6588	225.56	232.83
97	778.0	30.78	229.65	226.9795	−1.1629	224.43	231.68
125	778.5	31.22	229.65	231.0067	0.5908	228.50	235.85
160	778.7	31.22	229.65	231.4815	0.7975	229.01	236.37
188	777.2	28.55	211.60	210.0259	−0.7439	207.46	214.31
223	778.6	30.33	222.75	224.9212	0.9747	222.45	229.66
243	779.3	31.22	233.05	232.3911	−0.2827	229.98	237.36
298	779.2	30.67	228.65	228.3803	−0.1179	225.98	233.26
321	779.3	30.76	227.64	229.2991	0.7288	226.91	234.21
398	786.9	42.35	317.30	324.8447	2.3778	323.03	332.43
425	787.0	42.32	317.94	324.7715	2.1487	322.97	332.36
461	787.3	42.32	317.94	324.9876	2.2166	323.21	332.59
490	787.5	42.32	317.94	325.1511	2.2681	323.39	332.77
524	787.7	42.32	313.09	325.3321	3.9101	323.59	332.96
567	787.0	42.54	317.94	327.3489	2.9593	325.64	335.03
610	787.2	42.54	313.90	327.5484	4.3480	325.86	335.25
717	785.8	37.86	286.15	289.6324	1.2170	287.76	296.34
771	786.5	38.51	282.10	295.1652	4.6314	293.35	302.02

Table 5. The Optimized Results of SMR

no.	decision variables	nonoptimized values[19]	min. values	max. values	optimized values
1	catalyst mass distribution for the 1st reactor (weight fraction)	0.2	0.01	0.98	0.17
2	catalyst mass distribution for the 2nd reactor (weight fraction)	0.3	0.01	0.98	0.25
3	catalyst mass distribution for the 3rd reactor (weight fraction)	0.5	0.01	0.98	0.58
4	compressor discharge pressure to the 1st reactor (kPa)	3703	2000	3703	3702.0
5	L_1/R for the 1st reactor	0.8	0.6	0.9	0.71
6	L_2/R for the 1st reactor	0.8	0.6	0.9	0.73
7	L_1/R for the 2nd reactor	0.8	0.6	0.9	0.71
8	L_2/R for the 2nd reactor	0.8	0.6	0.9	0.70
9	L_1/R for the 3rd reactor	0.8	0.6	0.9	0.71
10	L_2/R for the 3rd reactor	0.8	0.6	0.9	0.70
11	the fraction of the total sweep gas to the 1st reactor	0.333	0.01	0.98	0.26
12	the fraction of the total sweep gas to the 2nd reactor	0.333	0.01	0.98	0.47
13	the fraction of the total sweep gas to the 3rd reactor	0.333	0.01	0.98	0.27
14	membrane thickness of the 1st reactor (μm)	10	1	30	12
15	membrane thickness of the 2nd reactor (μm)	10	1	30	28
16	membrane thickness of the 3rd reactor (μm)	10	1	30	29
17	sweep gas pressure for the 1st reactor (kPa)	985	100	1000	242.0
18	sweep gas pressure for the 2nd reactor (kPa)	1810	101	1000	563.0
19	sweep gas pressure for the 3rd reactor (kPa)	2000	101	1000	797.0
20	total molar flow rate of sweep gas (kmol/h)	1000	101	1000	387.87
21	hydraulic diameter for the 1st reactor (m)	0.1	0.05	0.5	0.35
22	hydraulic diameter for the 2nd reactor (m)	0.1	0.05	0.5	0.30
23	hydraulic diameter for the 3rd reactor (m)	0.1	0.05	0.5	0.19
24	hydrogen mole fraction in the recycled stream	0.695	0.5	0.75	0.52
25	hydrogen mole fraction in the sweeping gas	0.695	0	0.95	0.84
26	total fresh naphtha feed to the 1st reactor	266.74	200	350	267.83

Twenty six decision variables including operating conditions and design parameters are considered during the optimization process. The minimum and maximum values as well as the optimized values of the decision variables are reported in Table 5. It is worth noting

dx.doi.org/10.1021/ie2010912 |*Ind. Eng. Chem. Res.* 2012, 51, 398–409

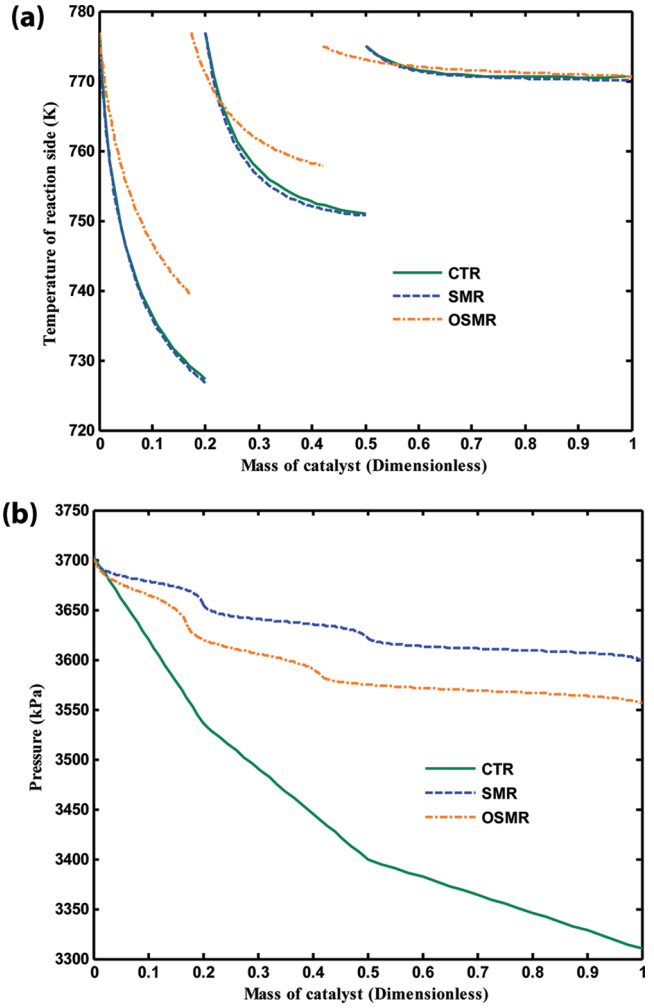

Figure 4. (a) The reaction side temperature profiles and (b) the pressure profile along CTR, SMR, and optimized SMR (OSMR).

that the optimization is carried out from the process viewpoint and costs are not considered in the optimization procedures mainly due to lack of additional cost data.

8. RESULTS AND DISCUSSION

In this section, the superior performance of optimized SMR configuration to that of nonoptimized SMR and CTR is clarified. Some advantages of spherical configurations (both optimized and nonoptimized reactors) over CTR and TMR are as follow:

(1) the feasibility of utilizing smaller catalytic pellets with higher effectiveness factor compared with the tubular reactors (CTR and TMR) mainly due to lower pressure drop in spherical configurations
(2) a significant reduction in the provided power supply for OSMR permeation side compared with SMR
(3) lower required material in spherical reactors compared with the tubular ones (material thickness for a spherical and a tubular pipe of the same radius, subjected to action of an internal pressure (P), are $t_{sph} = Pr/(2\sigma)$ and $t_{tub} = Pr/\sigma$, respectively, where t is the wall thickness, σ is the tensile stress, and r is the radius of the tube and the sphere[15])
(4) operating at higher flow ratios in spherical reactors (the feasibility of an augmentation in the inlet molar flow rate) without a significant pressure drop (the spherical configurations have higher production rate in a constant aromatic or hydrogen yield compared with the tubular reactor)[16]
(5) a sharp decline in the membrane surface in use and the related costs in SMR compared with TMR (the total membrane areas for TMR, SMR, and OSMR are 116.4, 69.35, and 65.4 m^2, respectively)

8.1. Steady-State Optimization. The performance of SMR under optimized operating conditions is investigated in the following figures and compared with the performances of nonoptimized SMR and CTR. Since the operating pressure and the temperature profile of the reaction side play a significant role in the enhancement of main products yield and generally in the reactor performance, they are investigated first.

The reaction side temperature profile along CTR, SMR, and OSMR is illustrated in Figure 4a. Since naphtha reforming reactions are predominantly endothermic, the reaction-side temperature decreases abruptly along the reactors. Since the naphtha feed concentration is high at the inlet of the first reactor, the reactions take place well and the temperature significantly drops. However, the reaction rate decreases at the end of the first reactor owing to a decrease in the reaction side temperature. Consequently, the outlet stream from the first reactor is preheated via a furnace before entering the second reactor. In the second reactor, the same abrupt temperature drop similar to the first reactor is not observed because the most concentration of the naphtha feed has been consumed in the first reactor which decreases the reaction rates in the second reactor. Ultimately, the lowest temperature drop is achieved in the third reactor due to the least concentration of the naphtha feed and the proceeding of the reactions along the reactor.

A reaction-side temperature drop in OSMR is considerably lower than the one in CTR and SMR because higher molar flow rate of the sweeping gas in OSMR acts as an external heating medium for the reaction side. The hydrogen mole fraction in the recycled stream is considered variable during the optimization step. According to Table 5, the hydrogen mole fraction in the recycled stream decreases from 0.695 (the inlet value for none optimized condition) to 0.53 (in the optimized condition); therefore the recycled stream molar flow rate should be increased to maintain H_2/HC at the inlet value of 4.73 (H_2/HC is an important operating factor which should be adjusted at the reactor entrance in order to reduce the catalyst burden and avoid rapid coking on the catalyst surface. It is recommended in the naphtha reforming process to maintain the H_2/HC molar ratio in the range of 4−6[14] in order to reduce coking and prevent a huge load on the catalyst during the operation). This increase in the amount of the recycled stream causes a decrease in the temperature drop along the reactor.

In the gas-phase reactions, the concentration of reactants is significantly affected by changes in the total pressure. Indeed, the reaction rates and conversions are strongly reduced as well as total pressure. Consequently, proper accounting for the effects of pressure drop in the reactors, in many instances, is a key issue in the success or failure of the reactor operation. Furthermore, using larger catalyst particles increases the intraparticle diffusion effects and the required time for a given number of reactant and product molecules to diffuse in and out the catalyst particle where they undergo reaction.[12] The pressure profile is depicted in Figure 4b.

dx.doi.org/10.1021/ie2010912 |*Ind. Eng. Chem. Res.* 2012, 51, 398–409

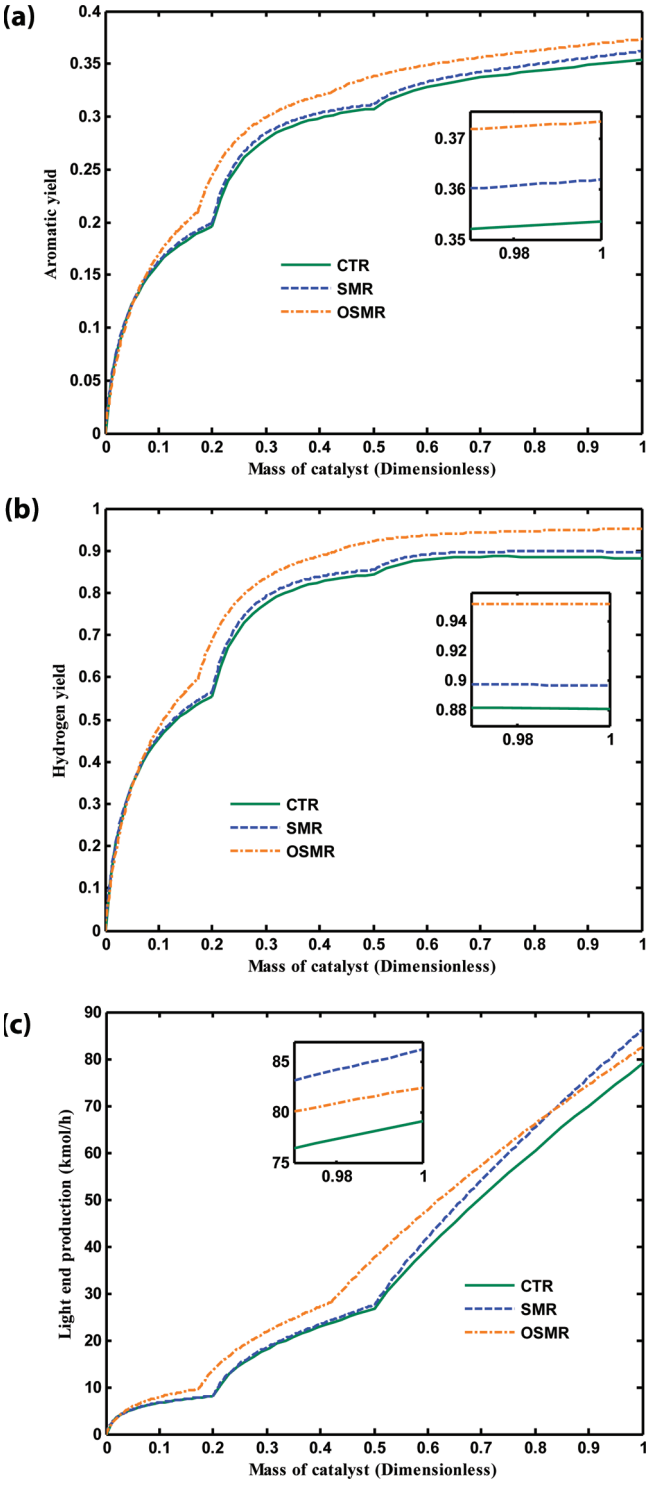

Figure 5. (a) The aromatic yield, (b) hydrogen yield, (c) the light ends production along CTR, SMR, and OSMR.

As seen, the pressure drop along spherical reactors is considerably lower than the one along CTR. The pressure drop along OSMR is slightly higher than the one along SMR owing to an increase in the recycled gas stream molar flow rate under the optimized conditions. According to the Ergun's equation, the pressure drop along the reactor has a direct relationship with the inlet molar flow rate where higher values of the recycled stream

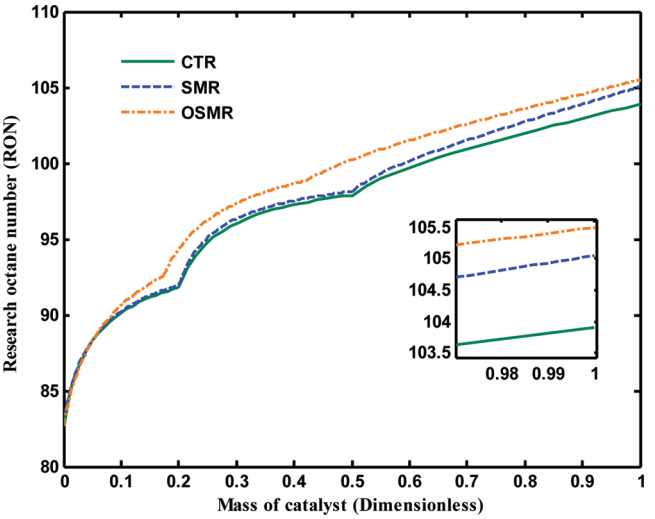

Figure 6. The research octane number along CTR, SMR, and OSMR.

molar flow rate in OSMR cause higher pressure drop along OSMR compared with SMR.

The legislative requirements for sulfur removal from gasoline and diesel have increased hydrogen use in refineries; therefore, they are looking for ways to maximize their hydrogen yields.[1] Furthermore, the increasing demand for high octane gasoline motivates refineries to devise some new technologies and fundamental changes in their available complex. The aromatic and hydrogen yields along CTR, nonoptimized SMR and OSMR are illustrated in Figure 5a,b. As seen, the aromatic and hydrogen yields along OSMR are considerably higher than the ones along CTR and SMR. Operating under optimized conditions and the in situ hydrogen removal enhance the aromatic and hydrogen yields in OSMR. The in situ hydrogen removal shifts the first reaction to the products side as well as the second reaction to the reactants side according to Le Chatelier's principle which enhances the aromatic and hydrogen yields in membrane reactors. Furthermore, higher temperature of the sweeping gas in the shell side of OSMR operates as an external heating medium. The small graph in Figure 5b reveals that hydrogen is progressively produced along the third reactor of OSMR (even up to the end of the reactor) unlike CTR where hydrogen is consumed at the end of the third reactor (see Figure 1). According to Figure 5b, the hydrogen yield in the second reactor of OSMR is approximately higher than the one in CTR and SMR therefore it can be economical to operate under optimized conditions with two reactors of OSMR instead of three reactors of CTR and SMR. In fact, if the hydrogen production is the target of refineries, it is economical to eliminate the third reactor and operate under optimized conditions in SMR owing to high costs of catalysts and higher volume of the third reactor in comparison with those of the first and the second reactors.

Figure 5c implies the light ends production rate along three configurations. Lighter ends are achieved by the hydrocracking of paraffins and naphthenes. The light ends production rate in the first and the second reactors of OSMR is higher than the one in the other reactors however it becomes lower than the one in SMR at the end of the third reactor. A comparison between the results of Table 1 shows that the third and the fourth reactions proceed well along SMRs compared with CTR. Therefore,

dx.doi.org/10.1021/ie2010912 |*Ind. Eng. Chem. Res.* 2012, 51, 398–409

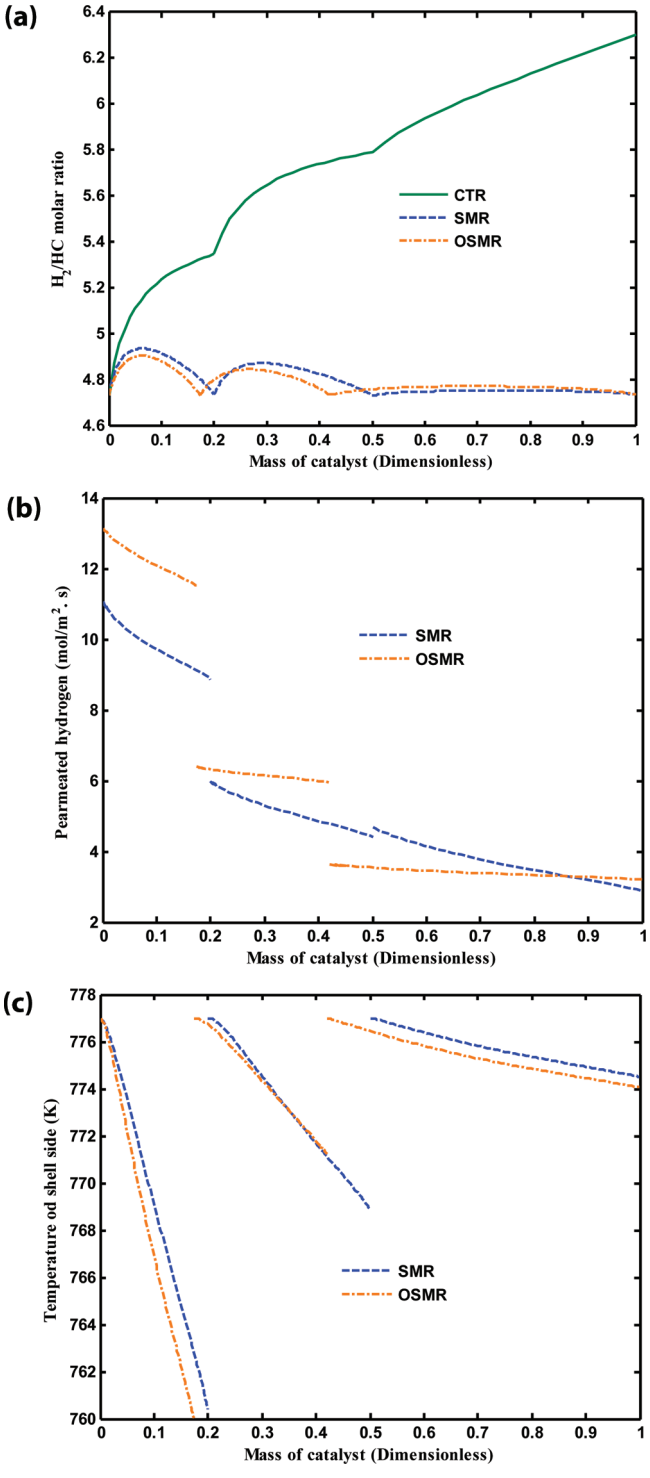

Figure 7. (a) The H_2/HC molar ratio along CTR, SMR and OSMR; (b) hydrogen permeation rate; (c) the temperature profile of the shell side along SMR and OSMR.

higher light ends production rate can be achieved in SMRs. Light ends are used as valuable feedstock for LPG production.

Reforming units provide significant advanced control opportunities because of the high value attached to reformate octane and hydrogen, expensive operating costs, and complex multivariable process interactions. RON characterizes unit severity and impacts on a whole range of other unit parameters that include product yield patterns, reactor temperatures, catalyst deactivation, and product composition. Therefore, reformate RON is a key measurement in any catalytic reformer control scheme. Higher reformate production rate (7.5 kmol/h compared with SMR) and the aromatic content of the reformate are achieved in OSMR. Consequently, OSMR can produce gasoline with higher octane number. The increase in the aromatic content of the reformate in OSMR improves the gasoline RON. Figure 6 shows the successful enhancement in octane number in OSMR. RON is calculated based on considering the aromatics, naphthenes, and paraffins as three pseudocomponents. The RON of each pseudocomponent evaluated by averaging the detailed RON of components is defined in the literature.[1,17]

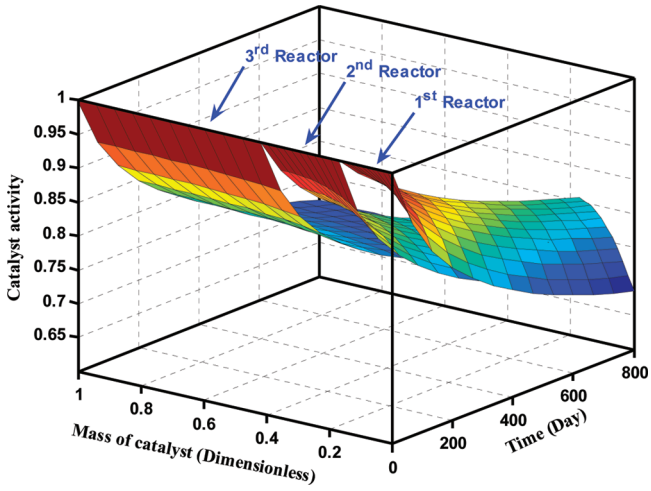

Figure 8. The catalyst activity as a function of time and the length of OSMR.

The H_2/HC molar ratio, in the reaction side, along three configurations is depicted in Figure 7a. It increases drastically along CTR owing to continuous hydrogen production along the reactor which reduces the aromatic and hydrogen production. On the other hand, the membrane layer maintains H_2/HC molar ratio at approximately the inlet value. The hydrogen permeation rate through the Pd−Ag membrane layers of SMR and OSMR is illustrated in Figure 7b. The hydrogen permeation rate through the first and the second reactors of OSMR is higher than the one in SMR which expresses the arrangement of H_2/HC ratios in Figure 7a.

The temperature profile of the shell side along SMR and OSMR is depicted in Figure 7c. The shell-side temperature along OSMR is lower than the one along nonoptimized SMR. A decrease from 1000 (nonoptimized value in SMR) to 387 (optimized value) in the sweeping gas molar flow rate (F_t) in OSMR causes an increase in the shell side temperature drop along OSMR compared with SMR. According to Figure 7b, higher hydrogen permeation rate in the first and the second reactors of OSMR contributes to considerably lower shell side temperature in OSMR as a result of lower reaction side temperature (permeated hydrogen) than the shell side temperature (i.e., heat transfer due to mass transfer).

The 3D plot of the catalyst activity as a function of time and the length of OSMR is shown in Figure 8. As seen, the catalyst activity deteriorates with time mainly due to coking and sintering phenomena. The catalyst has higher activity along the reactor. In fact, at lower temperatures, the probability of the catalyst deactivation by coking and sintering phenomena decreases.

dx.doi.org/10.1021/ie2010912 |*Ind. Eng. Chem. Res.* 2012, 51, 398–409

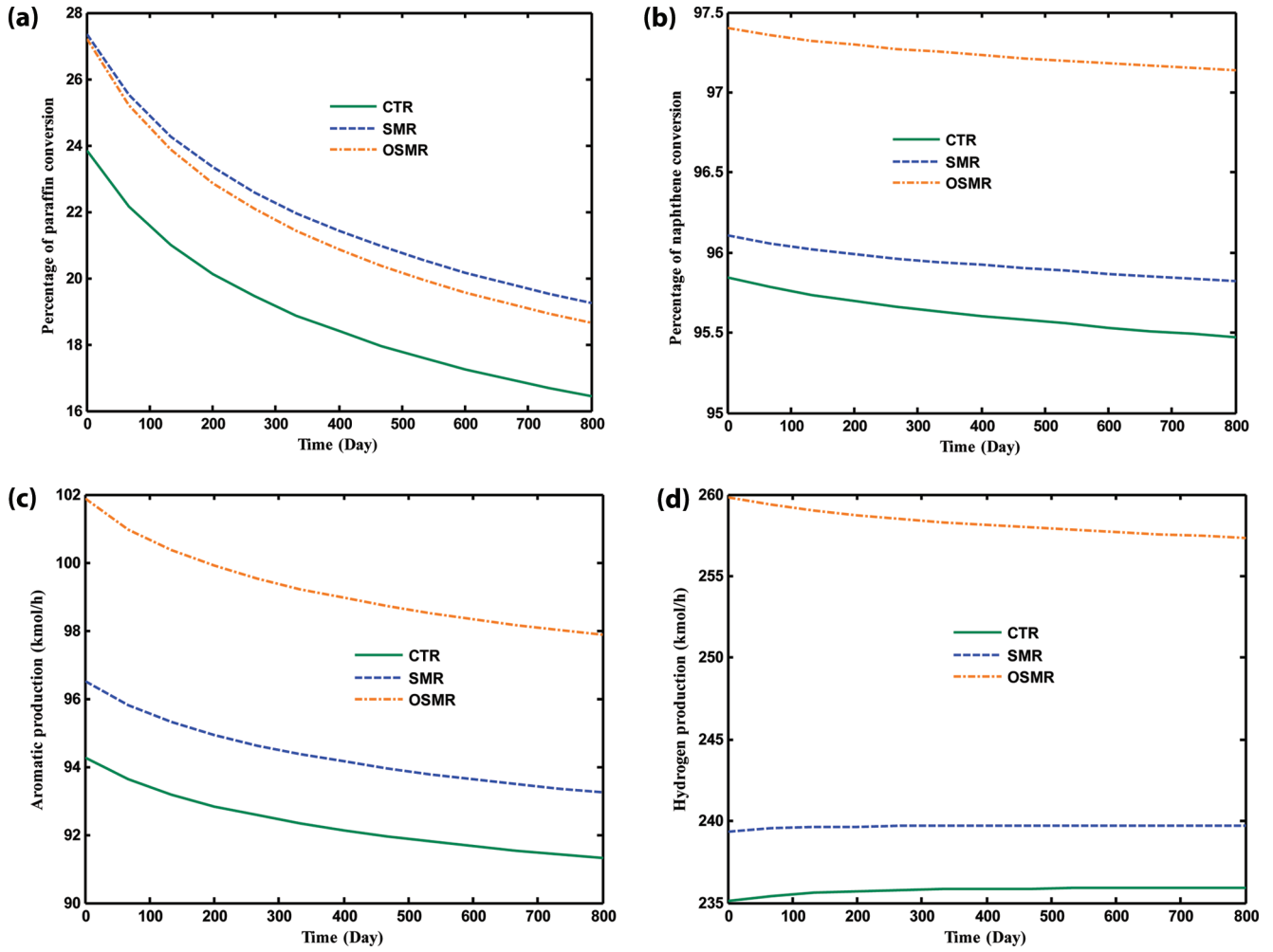

Figure 9. The percentage of (a) paraffin and (b) naphthene conversions and the production rates of (c) aromatics and (d) hydrogen along CTR, SMR, and OSMR for 800 days of operation.

8.2. Dynamic Optimization. In this section, the performnace of three configurations are investigated in the course of time (for 800 operating days) to evaluate the effect of catalyst deactivation on the products yield and the percentage converison of reactants. Note that these figures have been plotted by considering the total inlet fresh naphtha feed equal to 30.41×10^3 kg/h for all 800 days of operation just to show how the catalyst activity affects the production rates. In fact, the total fresh feed changes in the course of time due to the demands and downstream uses in refineries.

The percentage of paraffin and naphthene conversion and the production rates of aromatics and hydrogen are investigated with time in Figure 9a−d. As seen, a considerable decrease in the conversion of reactants and consequently in the products yield is observed mainly due to catalyst deactivation. The catalyst deactivation has an adverse effect on the above-mentioned issues in order that they decrease with time.

The variation of reformate production rate with time is investigated in Figure 10. The reformate production rate increases with time mainly due to the increase in the amount of unreacted paraffin and naphthenes. However, the aromatic content of reformate decreases with time as a consequence of catalyst deactivation which simultaneously decreases the aromatic production rate and increases the reformate production rate. Although the aromatic content of reformate (octane number) diminishes in the course of time, higher amount is achieved in OSMR than in other configurations (SMR and CTR).

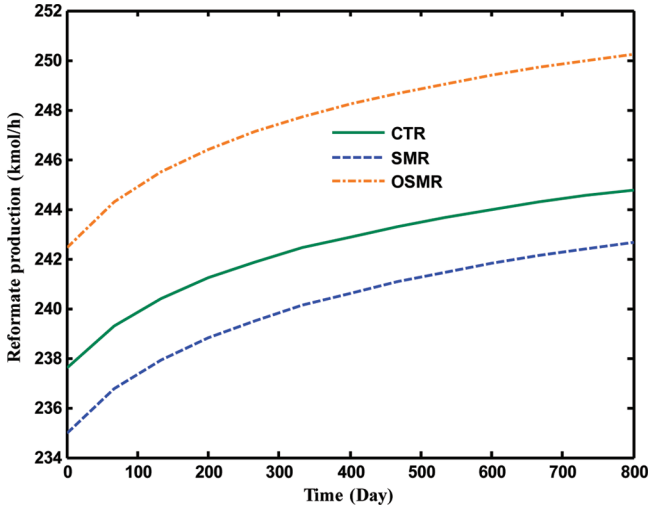

Figure 10. The variations of reformate production rate with time.

dx.doi.org/10.1021/ie2010912 |*Ind. Eng. Chem. Res.* 2012, 51, 398–409

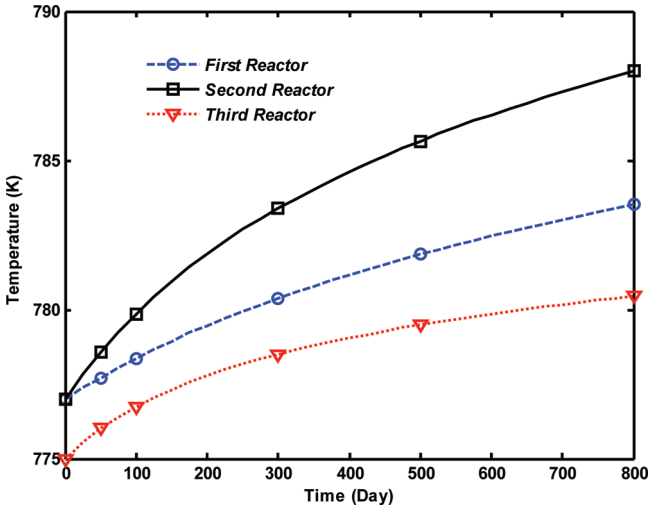

Figure 11. The optimized inlet temperatures of the first, the second, and the third reactors of OSMR for 800 operating days.

8.3. Time Trajectory. Due to a decrease in the percentage conversion of reactants and products yield with time by coking and sintering phenomena, the inlet temperatures of three reactors should be increased to compensate the undesired effect of catalyst deactivation. In other words, the inlet temperatures of the reactors are increased to achieve similar products yield to the values at the steady state condition ($t = 0$). The inlet temperatures of three reactors have been optimized in this regard. The decision variables in the unsteady-state condition are the first, the second, and the third reactors' temperatures (The time trajectory is evaluated based on the constant fresh naphtha feed $F = 30.41 \times 10^3$ kg/h). The objective function is defined as follows:

$$\mathrm{OF} = (Y_{H_2}^{t=t} - Y_{H_2}^{t=0})^2 + (Y_{\mathrm{aromatics}}^{t=t} - Y_{\mathrm{aromatics}}^{t=0})^2 \qquad (31)$$

The optimized inlet temperatures of the first, the second, and the third reactors in OSMR for 800 operating days are presented in Figure 11. As seen, the decrease in products yield and the percentage conversion of reactants owing to catalyst deactivation are compensated with increasing the inlet temperatures of three reactors with time.

9. CONCLUSIONS

The operating conditions of spherical membrane reactor (SMR) are optimized by the DE method to maximize the hydrogen yield, the reformate production rate, and the aromatic content of reformate (gasoline RON). Twenty six decision variables are considered to investigate the performance of SMR under optimized operating conditions and design variables. The optimization results show 8.33% and 6.25% increase in the hydrogen and the aromatic production rates. Moreover, nearly 550 kg/h additional gasoline can be achieved in OSMR in comparison with nonoptimized condition. Furthermore, a large saving in the operating costs is achieved owing to a remarkable decrease in the sweeping gas pressures under optimized conditions. Therefore, optimizing the operating conditions and design parameters of the spherical membrane reactors as a new generation of naphtha reactors provides more reliable and accurate insight into the future plant design. Moreover, as the optimization results show, the main recent needs of refineries for high gasoline RON, hydrogen production, and BTX production can be properly addressed by utilizing optimized SMR configuration. The costs evaluation of revamping the existing plant to the spherical membrane reactors, however, with the advantage of operating under optimum conditions, should be performed experimentally as a future work to obtain an entire judgment.

AUTHOR INFORMATION

Corresponding Author

*Tel.: +98 711 2303071. Fax: +98 711 6287294. E-mail address: rahimpor@shirazu.ac.ir.

NOMENCLATURE

a = catalyst activity
a_s = catalyst mass distribution,-
A = moles of aromatic formed, kmol h^{-1}
A_c = cross section between the inner and outer sphere, m^2
A_{c_1} = cross-section area of catalytic packed bed reactor (inner sphere), m^2
A_p = perimeter area of the inner sphere, m
b_s = sweeping flow distribution,-
C_j = concentration of component j, kmol m^{-3}
C_{j_0} = inlet concentration of component j, kmol m^{-3}
C_p = specific heat capacity, kJ $kmol^{-1}$ K^{-1}
d_p = particle diameter, m
D_{e_j} = effective diffusivity of component j, $m^2 s^{-1}$
D_H = hydraulic diameter, m
D_{i_m} = diffusivity of component i in the gas mixture, m^2 s^{-1}
E_d = activation energy of catalyst, J mol^{-1}
E_i = activation energy for i^{th} reaction, kJ $kmol^{-1}$
h_f = heat transfer coefficient, W m^{-2} K^{-1}
HC = hydrocarbon, kmol h^{-1}
H_2 = hydrogen, kmol h^{-1}
k_{eff} = effective thermal conductivity, W m^{-1} s^{-1}
k_{c_i} = mass transfer coefficient for component i, m h^{-1}
K_d = deactivation constant of the catalyst, h^{-1}
L = length of reactor, m
m = number of reaction
m_c = mass of catalyst, kg
M_i = molecular weight of component i, kg $kmol^{-1}$
M_w = average molecular weight of the feedstock, kg $kmol^{-1}$
n = number of component
N_A = molar flow rate of aromatic, kmol h^{-1}
N_i = molar flow rate of component i, kmol h^{-1}
p = moles of paraffin formed, kmol h^{-1}
P_i = partial pressure of ith component, kPa
P = total pressure, kPa
Q = volumetric flow rate, $m^3 s^{-1}$
R = radius, m
r_i = rate of i^{th} reaction, kmol $kgcat^{-1}$ h^{-1}
R = gas constant, kJ $kmol^{-1}$ K^{-1}
s_a = specific surface area of catalyst pellet, m^2 kg^{-1}
t = time, h
T = temperature of gas phase, K
T_{ref} = reference temperature, K
u_z = axial velocity, m s^{-1}
y_i = mole fraction for ith component in gas phase
z = variable represent length of reactor, m

Greek Letters

ε = void fraction of catalyst bed
μ = viscosity of gas phase, kg m^{-1} s^{-1}

v_{ij} = stoichiometric coefficient of component i in reaction j
ρ = density of gas phase, kg m^{-3}
ρ_b = catalyst bulk density, kg m^{-3}
σ = tensile stress, Nm^{-2}
ϕ_s = sphericity
ΔH = heat of reaction, kJ $kmol^{-1}$ of H_2

Subscript

a = aromatic
h = hydrogen
i = numerator for reaction
in = input
j = numerator for component
n = naphthene
out = outlet
p = paraffin
ss = steady state

Definitions

CTR = conventional tubular reactor
MON = motor octane number
OF = objective function
OSMR = optimized spherical membrane reactor
Pt = platinum
Re = rhenium
RON = research octane number
SMR = spherical membrane reactor
sph = spherical reactor
TMR = tubular membrane reactor

REFERENCES

(1) Antos, G. A.; Aitani, A. M. *Catalytic Naphtha Reforming*; Marcel Dekker, Inc.: New York, 1995.
(2) Kardamakis, A.; Pasadakis, N. Autoregressive modeling of near-IR spectra and MLR to predict RON values of gasolines. *Fuel* **2010**, *89*, 158.
(3) Morgan, N.; Smallbone, A.; Bhave, A.; Kraft, M.; Cracknell, R.; Kalghatgi, G. Mapping surrogate gasoline compositions into RON/MON space. *Combust. Flame* **2010**, *157*, 1122.
(4) Rahimpour, M. R.; Iranshahi, D.; Pourazadi, E.; Paymooni, K.; Bahmanpour, A. M. The aromatic enhancement in the axial-flow spherical packed bed membrane naphtha reactors in the presence of the catalyst deactivation. *AIChE J.* **2011** DOI 10.1002/aic.12529.
(5) Kumar, A.; Gautami, G.; Khanam, S. Hydrogen distribution in the refinery using mathematical modeling. *Energy* **2010**, *35*, 3763.
(6) Price, K.; Storn, R.; Lampinen, J. A. *Differential Evolution, a Practical Approach to Global Optimization*; Springer: New York, 2005.
(7) Babu, B. V.; Angira, R. Optimal design of an auto-thermal ammonia synthesis reactor. *Comput. Chem. Eng.* **2005**, *29*, 1041.
(8) Vakili, R.; Setoodeh, P.; Pourazadi, E.; Iranshahi, D.; Rahimpour, M. R. Utilizing differential evolution (DE) technique to optimize operating conditions of an integrated thermally coupled direct DME synthesis reactor. *Chem. Eng. J.* **2011**, *168*, 321.
(9) Smith, R. B. Kinetic analysis of naphtha reforming with platinum catalyst. *Chem. Eng. Prog.* **1959**, *55*, 76.
(10) Khosravanipour Mostafazadeh, A.; Rahimpour, M. R. A membrane catalytic bed concept for naphtha reforming in the presence of catalyst deactivation. *Chem. Eng. Process.* **2009**, *48*, 683.
(11) Adhikari, S.; Fernando, S. Hydrogen Membrane Separation Techniques. *Ind. Eng. Chem. Res.* **2006**, *45*, 875.
(12) Fogler, H. S. *Elements of Chemical Reaction Engineering*, 2nd ed.; Prentice-Hall: Englewood Cliffs NJ: 1992.
(13) Iranshahi, D.; Rahimpour, M. R.; Asgari, A. A novel dynamic radial-flow, spherical-bed reactor concept for naphtha reforming in the presence of catalyst deactivation. *Int. J. Hydrogen Energy* **2010**, *35*, 6261.
(14) Operating Data of Catalytic Reformer Unit, Domestic Refinery. 2005.
(15) Streeter, V. L.; Wylie, E. B.; Bedford, K. W. *Fluid Mechanics*, WCB McGraw-Hill: Boston, 1998.
(16) Iranshahi, D.; Pourazadi, E.; Paymooni, K.; Bahmanpour, A. M.; Rahimpour, A. M.; Shariati, A. Modeling of an axial flow, spherical packed-bed reactor for naphtha reforming process in the presence of the catalyst deactivation. *Int. J. Hydrogen Energy* **2010**, *35*, 12784.
(17) American Institute Research Project 45, 16th annual report, 1954.